Structural Monitoring and Maintenance, *Vol. 12, No. 4 (2025) 395-415*
https://doi.org/10.12989/smm.2025.12.4.395

Failure detection in single plate shear connection with LSTM network

Priti R. Satarkar*[1], P.R. Dixit[2a], S.N. Londhe[2b] and Preeti S. Kulkarni[2c]

[1]*Department of Civil Engineering, All India Shri Shivaji Memorial Society, College of Engineering, Pune, India*
[2]*Department of Civil Engineering, Vishwakarma Institute of Information Technology, Pune, India*

(*Received April 6, 2025, Revised December 21, 2025, Accepted January 9, 2026*)

Abstract. The single plate shear (SPS) connection is a cost-effective choice for beam to column connections. The failure detection method for the connections helps people to respond and receive an early warning, allowing them to take action earlier and prevent serious consequences. Thus, a quick solution is needed to address the structural safety monitoring issue and predict the response of the SPS connection with accuracy and speed. The present study recommends the behaviour of SPS connection to predict its failure mode using long-short term memory (LSTM) networks. The LSTM models were designed utilising the datasets generated by applying a finite-element method (FEM) of SPS connection. Experimental Validated model was used for finite element analysis of 48 SPS connections with different seven parameters like distance, the depth of the shear plate connection plate, thickness of web, thickness of shear plate, the number of bolt columns, Grade of bolts, the beam span, and a number of common wide flange beam shapes. The LSTM model utilise von Mises stresses for analysing the failure mode of the SPS connection was compared to the results of the artificial neural network (ANN) and the FEM. The output of an LSTM model was nearly identical to an ANN model, with ANN model performing slightly better. In all three outputs, the ANN model's performance is satisfactory ($r > 0.8$). The training and testing of the ANN models required an average of six seconds, whereas the analysis of the deep LSTM network consumed almost an hour. The comparison shows that the ANN model predicted stresses more accurately than LSTM, at least for the current work, which reduces the necessity of using LSTM for the said task.

Keywords: artificial neural network (ANN); finite element analysis; long-short term memory (LSTM); single plate shear connection; steel structures

1. Introduction

Studies have showed that beam to column connections are the primary means of load transmission in the building, making connection between them is one of the most significant aspects of building constructions. These days it seems that steel structures are growing in popularity in industrial as well as in residential building than concrete structures. The single plate

*Corresponding author, Assistant Professor, E-mail: prsatarkar@aissmscoe.com
[a] Ph.D., E-mail: pradnya.dixit@viit.ac.in
[b] Ph.D., E-mail: shreenivas.londhe@viit.ac.in
[b] Ph.D., E-mail: preeti.kulkarni@viit.ac.in

 ISSN: 2288-6605 (Print), 2288-6613 (Online)

shear connection (SPS) is a cost-effective solution for beam to beam or beam to column web connections which does not require copes and is simpler and safer to install (Gong 2010, Yura and Summers 1982). For these reasons the research in SPS connections began to attract attention. Fig. 1 shows a schematic diagram of SPS Connection.

The single plate is unstable and may cause out-of-plane movement because of its extended length. A number of experiments conducted by Sherman and Ghorbanpoor (2002), excessive twisting of the SPS connections was identified. According to the results, they recommended that SPS connections be avoided unless stiffeners or stabilizer plates were placed in the joint location and that twisting would need to be taken into consideration. The AISC Steel Construction Manual (2010), includes equations to assess the requirement for stiffeners. The capacities based on AISC proved to be lesser than the measured values in eight full-scale SPS connections tested by Creech (2005) and Kirsten and Metzger (2006). This suggests that the AISC Steel Manual's method is conservative Due to large discrepancy among the theoretical analysis and actual behaviour of steel structures, the connections are complex to analyze and design. Various geometric properties of connecting parts materials make it difficult to conduct experiments under all loading conditions. It also takes a lot of time as well as money, and is unable to completely assess the effects of every parameter.

Therefore, these problems can be resolved with the use of simulation programmes (Finite Element Analysis). Determining a structure's displacements, strain and stresses under a given set of loads can be done effectively with the use of finite element analysis (FEA) (Suleiman 2013). The FEA can be used to determine the damages and failures of structures. FEA models typically include complex processes and lengthy computing time to get final simulation outcomes. To account for nonlinearity, the processes need discretizing the various connection components (Column, Beam, shear tab and Bolts) into finite elements along both span directions and/or throughout the depth or thickness (Singh *et al.* 2021). Razavi and Hadidi (2020) examined, from a unique perspective, the effectiveness and suitability of a sensitivity-based FE model update framework for identifying damage in large-sized structures. These techniques are precise but require a significant amount of computing work and are therefore unsuitable for use by practicing engineers in everyday design. This necessitates the use of an alternative method that will produce acceptable accuracy and allow for quick assessment of the SPS connection's failure mode. There has been a growing interest in using Artificial neural networks (ANNs) and Deep learning methods like convolutional neural network (CNN) and long short-term memory (LSTM) network in structural engineering. In object detection, convolutional neural networks (CNNs) a deep learning technique, proved their effectiveness, (Zhao *et al*. 1998). In comparison to traditional machine learning techniques, deep learning (DL) can automatically detect objects and learn features on their own without the need for hand-crafted features, (Rosebrock 2017). There are various case studies available on DL for crack detection, including those on masonry walls (Dais *et al*. 2021) and inspection of bridges, tunnels, and pavement by (Savino and Tondolo 2021). The long short-term memory (LSTM) neural network is one of the advanced applications of deep learning (DL). It has been successfully used in a variety of fields, especially sequence problems, including speech recognition, machine translation, language modelling, rainfall-runoff simulation, and structural health monitoring. Based on these advancements, Long Short-Term Memory (LSTM) networks in particular have drawn more interest because of their long-term dependencies in sequential data, which are challenging for conventional ANNs to learn since the gradient becomes very small and obstructs learning. LSTMs overcome these problems by addressing the vanishing gradient problem that can arise in deep networks during training. LSTM-based models have been successfully

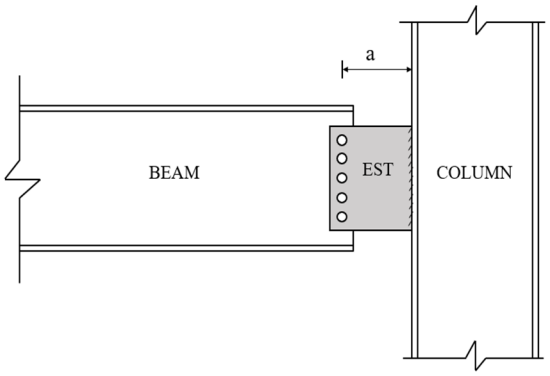

Fig. 1 Schematic Diagram of single plate Shear Connection

implemented in a number of areas and can be useful for failure analysis prediction. In this regard, the suggested deep LSTM model-based approach for SPS connection failure detection fits in well with the broader deep learning-based SHM trend. The use of ANN and LSTM to structural engineering problems is described in the next section.

2. Literature review:

Good flexibility, adaptability, less complexity and computational costs are the unique advantages of neural network-based models. With advances in computer science, ANN has solved many structural engineering problems, such as load carrying capacity and shear strength prediction in different members of RCC structures by developing neural network models (Mansour *et al.* 2004, Tohidi and sharifi 2016, Kotsovu *et al*. 2017, Allahyari *et al*. 2018, Murad *et al*. 2020, Abambres and Lantsoght 2020, Limbachiya and Shamass 2021). Lima *et al.* (2005) suggested artificial neural networks with the back propagation supervised learning algorithm to predict the initial stiffness and flexural resistance of beam to column steel joints. Mazloom *et al*. (2018) used artificial neural networks and genetic algorithms to evaluate the ductility of moment frames. Nguyen *et al.* (2018) executed vibration-based artificial neural networks (ANNs) to numerically quantify damage in wind turbine towers. In structural engineering, concrete is also seen as an unsustainable product because of the substantial amount of cement used in its production. This is because the production of cement produces a lot of carbon emissions, mostly from the calcination of limestone and the burning of fuel. Thilakarathna *et al*. (2020) conducted an analysis to estimate the embodied carbon emissions of six high-strength concrete (HSC) mix designs. Their model achieved an accuracy of 97% using the ANN method, demonstrating its capacity to detect high-strength RMC mixtures while reducing the composition's embodied carbon footprint. In order to optimise the compressive strength prediction of alkaline-activated slag concrete (AASC) and offer a low-carbon substitute for conventional concrete, Tang *et al*. (2022) created four machine learning models based on ANN algorithms with different configurations. In order to address the embedded carbon emissions assessment difficulty in RMC production within the construction sector, Nguyen *et al.* (2025) used web crawling and natural language processing approaches to create a meta-dataset of more than 59,000 high-quality environmental product declarations records from North

America. To predict embodied carbon emissions in RMC goods, a meta-learning model based on the Model-Agnostic Meta-Learning algorithm was created. In terms of practical application, the trained model showed strong generalisation performance. Fils *et al*. (2021) developed a crack monitoring architecture based on Artificial Neural Networks (ANNs) as the machine learning algorithm, and its results are compared with a baseline model. Ahmed *et al.* (2022) used a data-driven machine learning (ML) framework to predict the ultimate shear strength and failure mechanisms of reinforced concrete ledge beams. Ho *et al*. (2022) suggested a technique that combines artificial neural networks (ANN) and electro-mechanical impedance (EMI) responses to identify cracks in metal structures. Tariq *et al*. (2022), focused on predicting the failure mode of steel flush end plate connection by using artificial neural networks (ANN's). Satarkar *et al.* (2023), suggested the use of artificial neural networks to predict the failure mode of SPS connection.

However, the information regarding the sequential order of the model inputs is lost, which is a drawback of feed-forward ANNs. Recurrent neural networks (RNNs), a type of deep learning algorithms, have gained popularity in recent years for their ability to solve sequential problems (Bergen *et al.* 2019). RNN was developed especially to study sequential, time-varying, linear/nonlinear patterns for regression issues (Medsker and Jain 1999, Mandic and Chambers 2001), showed a great potential for structural response modelling. Unfortunately, because of its architecture, it is unable to overcome the vanishing gradient problem and cannot therefore learn long-term consequential information. Long short-term memory (LSTM) networks are a unique kind of neural network with a state-of-the-art network architecture that can avoid the vanishing gradient issue. LSTM neural network was initially suggested by Hochreiter and Schmidhuber (1997). A few unique characteristics were added by the LSTM algorithm, such as the "forget gate," which helps the network successfully capture sequential dependencies and differentiates it apart from conventional RNNs. A detailed systematic review of LSTM-based SHM is, as illustrated below.

Zhang *et al*. (2019) presented an in-depth evaluation of the development of LSTM methods for modelling and predicting nonlinear structural responses. Liu et al. (2020) suggested the long short-term memory (LSTM) network-based recovery method for missing structural temperature data. Xue and Ou (2021) predicted the wind-induced nonlinear structure dynamic response by LSTM approach and applied to the transmission tower line system. Choe *et al*. (2021) introduced and evaluated a sequence-based deep learning (DL) modelling approach that combines LSTM and GRU neural networks for detecting structural damage in floating offshore wind turbine blades. Butta *et al*. (2022) provides an efficient load prediction system projected for different local feeders to predict the Medium- and Long-term Load Forecasting. Ranjbar and Toufigh (2022) developed a deep learning method for ultrasonic-based distributed damage analysis in concrete by utilising LSTM. Additionally, the LSTM models' performance was assessed in noisy conditions. The time series of the response signals were utilised by the suggested LSTM models in this study to evaluate damage. As a result, the LSTM layers automatically received the damage-sensitive features. Yan *et al.* (2023) presented an effective technique based on an LSTM neural network for the prediction of the time series of the top tension reaction of an umbilical cable. Zhang and Zhou (2023) suggested an intelligent identification method for the real-time monitoring of moving load active on bridges with the help of LSTM. He and Chen (2023) used LSTM to predict rock deformation around tunnels. Zhao *et al*. (2023) proposed an algorithm using a LSTM network to predict the wind-induced damage to lightning rod structures at varying wind speeds. Sharma and Sen (2023) proposed a real-time LSTM based method that uses an unsupervised LSTM prediction network to identify structural damage and a supervised classifier network for localization. Cha *et*

al. (2023), presented DNoiseNet, a deep learning–based feedback active noise control (ANC) system, to handle nonlinear and non-stationary noise in difficult situations like construction sites, vehicle interiors, and aeroplane cockpits. This work highlights the adaptability of deep learning in the structural and construction domains by showing how experienced deep learning operators can handle complicated, real-world noise control challenges.

As mentioned in the introduction and the literature review mentioned above, there are many deep learning techniques, such as CNN and LSTM, but in this study, LSTM was chosen due to its benefits. LSTM networks are a form of RNN architecture designed to solve certain limitations of conventional feedforward artificial neural networks. Long-term dependencies in sequential data are difficult for conventional ANNs to learn because the gradient becomes very small and obstructs learning. LSTMs overcome these problems by addressing the vanishing gradient problem that can arise in deep networks during training. The main reason for choosing LSTM is the structural response data utilised in this research is the failure progression in SPS connections changes sequentially with loading. LSTM networks have been developed specifically for studying temporal dependencies, long-term correlations, and nonlinear pattern of evolution in sequential data, in contrast to CNNs or conventional feedforward ANNs, which handle the input as independent observations. LSTM models retain information through memory cells and gate mechanisms. This enables them to learn how the structural behaviour changes as it approaches failure. CNNs work well for images (such as damage detection) and concentrate on spatial feature extraction, but they are not the most effective for modelling long term data degradation patterns. In a similar vein, basic ANNs do not have the inside memory structure required to record sequential behaviour. On the other hand, as demonstrated by a number of earlier research, including DNoiseNet (Cha *et al.* 2023), LSTM has been extensively used in structural health monitoring, active noise management, and other engineering domains where temporal behavioural analysis is important. As of now, failure analysis of steel connection has not explored by LSTM. With this view, in this research the results of ANN and LSTM are compared for prediction of failure mode of SPS connection.

The primary innovation of the current work lies in its methodology for failure detection of SPS connection joint. All the studies mentioned in the literature review have not dwelled into such deep comparisons. However, the literature generally focuses on either global beam–column system behavior or binary damage classification. None of the recent studies specifically address multi-class failure mode detection at the level of a steel SPS connection, which involves distinct local mechanisms such as bolt shear, plate yielding, and bearing failures. The present study addresses a significant gap in the literature by providing a particular methodology for identifying and differentiating failure modes in SPS connections where such robust, mode-specific characterisation has not yet been investigated. The SPS connection, which shows different failure modes has received very little attention. In order to facilitate this level of analysis, we create an extensive dataset that includes experimentally verified failure modes specific to shear-plate behaviour, enabling real multi-class identification instead of the conventional binary classification of damaged versus undamaged. To predict the failure modes of the SPS connection, 48 finite element models were developed in ABAQUS and produced the von mises stresses readings up to the ultimate load for each increment of load. In order to improve the accuracy, understanding, and usefulness of the suggested failure-mode detection methodology, developed a LSTM network that is reinforced by a carefully designed feature set that isolates the specific behavioural indications connected to each failure mode. A brief explanation of LSTM techniques is given in the next section. This is followed by a section devoted to the LSTM model development in the present

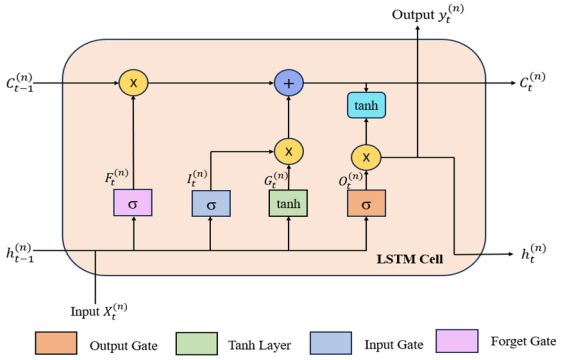

Fig. 2 Structure diagram of the nth LSTM cell hidden layer at time t

work. The LSTM results are shown in the results and discussion section. Concluding remarks concerning the current work are made at the end of the paper.

3. Deep Learning - Long Short-Term Memory (LSTM)

Hochreiter and Schmidhuber (1997) introduced LSTM, a variant of RNN, to solve the vanishing gradient problem in the conventional RNN model. The core concept of LSTM is the use of gate structures to regulate the state of information transmission, allow the network to selectively forget irrelevant information and recall necessary long-term memory information, and eliminate long series dependence in neural networks. The LSTM model can effectively solve long sequence problems with long-term dependencies by developing "gate" units such as input gates, output gates and forget gates as highlighted in Fig. 2, that the conventional RNN model is not able to reasonably solve because of problems like gradient disappearance and explosion. Through the three "gate" structures, the LSTM method introduces the unit memory cell C_t using a similar activation function σ. Overall, across time, the cell state C_t and hidden state h_t flow in parallel. The LSTM method can remember and forget data because to this well-developed "gate" structure (Smagulova and James 2019, Bakhshi *et al.* 2023).

The information that the LSTM unit needs to keep and forget from the cell state C_t is determined by the forget gate, which has the ability to selectively forget the last several sets of states and adjust the parameters. The forget gate operates by examining the output vector C_{t-1} from the preceding LSTM unit, combining the parameter h_{t-1} from the preceding time step with the input value X_t of the current time step, and producing a number between 0 and 1 through the activation function σ, also known as the sigmoid function. A value of 0 indicates to completely forget it, while a value of 1 indicates to keep it completely. Information screening is then accomplished by combining the product with C_{t-1}. The σ function and the tanh function are the two activation functions present in the input gate. Using the two activation functions mentioned earlier, the input X_t at the current time step and the hidden state h_{t-1} sent from the prior time step may be combined to generate the two activation vectors, I_t and G_t. In this case, G_t is also referred to as a candidate memory cell, and the cell state C_t medium gains its information from it. After activation, the output gate uses the functional values of X_t and h_{t-1} along with the value of the state variable C_t to calculate the output h_t of the entire processing unit.

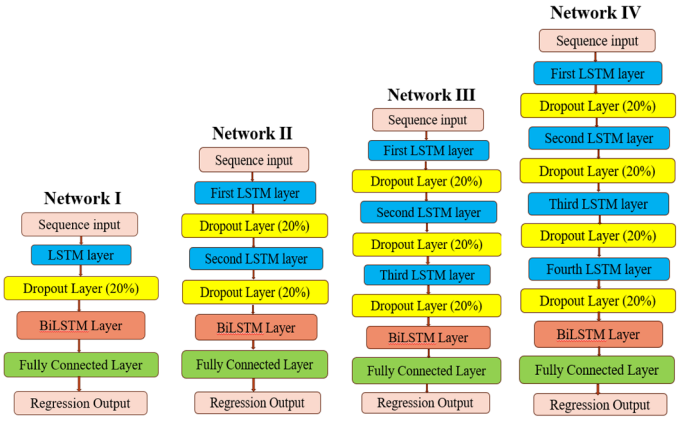

Fig. 3 Architecture of LSTM

3.1 Multi-hidden-layer LSTM structure

Input, output, and multiple LSTM layers are commonly present in a basic LSTM model. The number of hidden layers also increases the complexity of the nonlinear mapping relationship between the processing data samples. The iteration time and the number of LSTM hidden layers are positively correlated, and the calculation time grows exponentially with the number of hidden layers. However, this does not imply that the more hidden layers, the better the prediction for the unknown data. Apart from the aforementioned structure, the model data output is preceded by a Bidirectional LSTM (BiLSTM) and a fully connected (FC) layer situated between the output layer and the LSTM hidden layer. The appropriate output features are constructed by connecting the final multiple LSTM hidden layers to the target output layer through the FC layer. To further prevent overfitting during model training, a dropout layer, whose value usually varies between 0.2 and 0.5, can be added after each LSTM hidden layer (Zhang *et al.* 2019). In the field of deep learning, overfitting is a common issue.

The main concept of the dropout layer is to eliminate part of the data at a certain dropout rate and the mapping relationship between some variables is arbitrarily interrupted in the training process. Due to these factors, an LSTM model has much higher computation speed and efficiency. BiLSTM layers combine the two types of data scanning one forward and one backward to predict the output. Fig. 3 shows the architecture of LSTM network.

4. Data preparation for LSTM

One important factor that can impact both the LSTM's computing time and prediction accuracy is the size of the training dataset. A large dataset typically can obtain a promising prediction accuracy due to the strong generalization while more computing resources are involved in processing data. Here, LSTM model is designed for predicting SPS connection failure mode. FEM (ABAQUS software) was used to generate input and output values for the development of the LSTM model. To validate how precisely the FEM predicts the behaviour of the structure, the previously investigated specimens 3U and 4U were simulated in ABAQUS, which were examined experimentally by Sherman and Ghorbanpoor (2002). As stated by Ashakul (2004), Daniel and

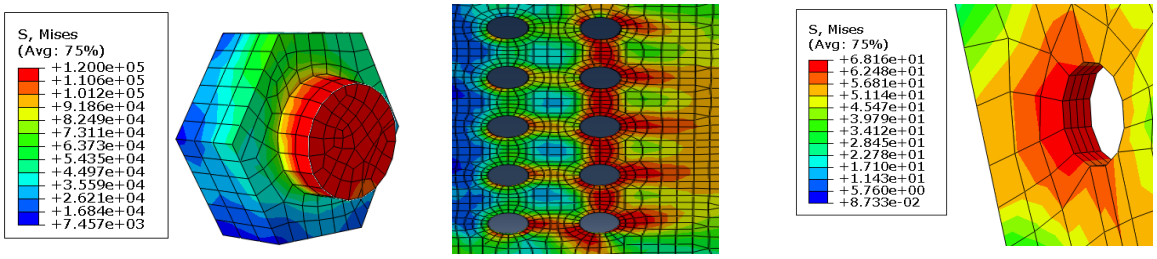

(a) (b) (c)

Fig. 4 Bolt shear failure, net shear-bending interaction and bolt bearing failure, Satarkar *et al*. (2023)

Ruffley (2011), the three-dimensional (3D) Solid Brick-Element was utilised. The beam and column were modelled using an 8-node brick element (C3D8R in ABAQUS), while a single shear plate was modelled using a 20-node brick element (C3D20R in ABAQUS). To optimise the mesh sizes, sensitivity studies were carried out (Creech 2004). Finer meshes were used to discretise the bolts, bolt holes and the beam within twice its depth along its length. For the remainder of the model, comparatively coarser meshes were utilised. One end of the beam is attached with a shear plate, while the other end is supported by a roller that is free to rotate but restrained in both the X and Y directions. A reference point was created in order to modeled the boundary condition. It uses ABAQUS's kinematic coupling constrain option to kinematically constrain all degrees of freedom on the surface of the beam's cross section. In the X, Y, and Z directions, the column's top and bottom nodes were restrained from moving. The shear plate is welded to column Flange, to model the weld line Tie constraint type was employed in the ABAQUS. In the X, Y, and Z directions, the bolt head was restrained. In order to allow the bolts to deform in response to the applied loads, this constraint must be deactivated and released throughout the loading phase. It is applied during the initial and pretension steps. For the structural component the yield strength (σy) and ultimate strength (σu) were taken as 345 (50 ksi) and 470 MPa (68 ksi), respectively. The Young's modulus (E) was cosidered as 200 GPa, and a value of 0.30 was utilized for Poisson's ratio (v). For A325 and A490 bolts, σu was set at 862 MPa (120 ksi) and 1138 MPa (150 ksi). The bolt shank was subjected to a temperature change in order to apply the minimum bolt pretension force prescribed by AISC (2010). A single load was applied at a distance of 1600 mm for 3U specimens and 915 mm for 4U specimens. The FEA results were verified using two types of measurements: comparing the connection's shear force with the angle of twist and its shear force with the vertical displacement along the bolt centre line. The FEM predicts capacity of connection and the measured responses such as the relationships between shear force and vertical deflection with an accuracy of 97.8% for 3U and 95.8% for 4U. The Finite element model predicts 89% accuracy of 4U model for the relationships between the shear force and angle of twist.

The results showed a high level of accuracy between the FEM and experimental results. The current authors have previously published validation graphs in Satarkar *et al.* (2023). In order to predict the mode of failure of the SPS connection, a total of 48 models (shown in Table 1) were developed in ABAQUS by changing different parameters. Table 1 compares the SPS connection failure mode according to AISC (2010) and FEA. Table 1 shows that the majority of failures for the SPS connections are bolt shear failure, net shear-bending interaction in the shear plate and bolt bearing failure, as illustrated in Fig. 4. Von Mises stress contours were compared with the ultimate bolt strength (Fu), which was taken to be 862 MPa (120 ksi), in order to computationally calculate

Table 1 Connection Details

Connection ID	Beam Size	Plate Dimensions				Bolt Information				Design Load / Udl	Failure Mode	
		a (mm)	tp (mm)	Depth (mm)	T (mm)	No of bolt column	No of bolts	db (mm)	dh (mm)		AISC (2010)	FEA
W18×35-229-1	W18×35	229	13	381	394	1	5	27	30	1.2	BB	BB
W21×44-229-1	W21×44	229	16	458	467	1	6	27	30	1.5	BB	BB
W24×62 -229-1	W24×62	229	16	434	528	1	7	27	30	1.5	BB	BB
W30×99 -229-1	W30×99	229	16	610	674	1	8	27	30	0.95	BB	BB
W18×35-229-2	W18×35	229	16	381	394	2	5	27	30	1.5	SBI	SBI
W21×44-229-2	W21×44	229	16	458	467	2	6	27	30	1.5	SBI	SBI
W24×62 -229-2	W24×62	229	16	434	528	2	7	27	30	1.5	SBI	SBI
W30×99 -229-2	W30×99	229	16	610	674	2	8	27	30	1.3	SBI	SBI
W18×35-280-1	W18×35	280	16	381	394	1	5	27	30	1.3	BB	BB
W21×44-280-1	W21×44	280	16	458	467	1	6	27	30	1.5	BB	BB
W24×62-280-1	W24×62	280	16	534	528	1	7	27	30	1.5	BB	BB
W30×99-280-1	W30×99	280	16	610	674	1	8	27	30	0.8	BB	BB
W18×35-280-2	W18×35	280	16	381	394	2	5	27	30	1.5	SBI	SBI
W21×44-280-2	W21×44	280	16	458	467	2	6	27	30	1.5	SBI	SBI
W24×62-280-2	W24×62	280	16	534	528	2	7	27	30	1.5	SBI	SBI
W30×99-280-2	W30×99	280	20	610	674	2	8	27	30	1.4	SBI	SBI
W16×26-229-1	W16×26	229	13	229	346	1	3	27	30	0.65	BB	BB
W16×57-229-1	W16×57	229	13	229	346	1	3	27	30	0.25	BB	BB
W18×35-229-1	W18×35	229	13	229	394	1	3	27	30	0.45	BB	BB
W18×86-229-1	W18×86	229	13	229	394	1	3	27	30	0.2	BF	BF
W21×44-229-1	W21×44	229	13	305	467	1	4	27	30	0.85	BB	BB
W21×93-229-1	W21×93	229	13	305	467	1	4	27	30	0.35	BF	BF
W24×62-229-1	W24×62	229	13	305	527	1	4	27	30	0.55	BB	BB
W24×103-229-1	W24×103	229	13	305	527	1	4	27	30	0.3	BF	BF
W30×99 -229-1	W30×99	229	16	381	673	1	5	27	30	0.4	BF	BF
W30×148-229-1	W30×148	229	16	381	673	1	5	27	30	0.4	BF	BF
W16×26-229-1	W16×26	229	13	305	346	1	4	27	30	1.5	BB	BB
W16×57 -229-1	W16×57	229	13	305	346	1	4	27	30	0.65	BB	BB
W18×86-229-1	W18×86	229	13	381	394	1	5	27	30	0.45	BF	BF
W21×93-229-1	W21×93	229	16	458	467	1	6	27	30	0.8	BF	BF
W24×103-229-1	W24×103	229	16	434	528	1	7	27	30	0.85	BF	BF
W30×148-229-1	W30×148	229	16	610	674	1	8	27	30	0.45	BF	BF
W16×26-280-1	W16×26	280	13	229	347	1	3	27	30	0.55	BB	BB
W16×57-280-1	W16×57	280	13	229	347	1	3	27	30	0.25	BB	BB
W18×35-280-1	W18×35	280	16	229	394	1	3	27	30	0.45	BB	BB
W18×86-280-1	W18×86	280	16	229	385	1	3	27	30	0.2	BF	BF
W21×44-280-1	W21×44	280	16	305	467	1	4	27	30	0.7	BB	BB
W21×93-280-1	W21×93	280	16	305	467	1	4	27	30	0.3	BF	BF
W24×62-280-1	W24×62	280	16	305	528	1	4	27	30	0.45	BB	BB
W24×103-280-1	W24×103	280	16	305	528	1	4	27	30	0.25	BF	BF
W30×99-280-1	W30×99	280	16	381	674	1	5	27	30	0.25	BF	BF
W30×148-280-1	W30×148	280	16	381	674	1	5	27	30	0.2	BF	BF
W16×26-280-1	W16×26	280	13	305	347	1	4	27	30	1	BB	BB
W16×57-280-1	W16×57	280	13	305	347	1	4	27	30	0.4	BB	BB
W18×86-280-1	W18×86	280	16	381	385	1	5	27	30	0.45	BF	BF
W21×93-280-1	W21×93	280	16	458	467	1	6	27	30	0.65	BF	BF
W24×103-280-1	W24×103	280	16	534	528	1	7	27	30	0.7	BF	BF
W30×148-280-1	W30×148	280	16	610	674	1	8	27	30	0.5	BF	BF

the bolt shear failure mode. A bolt shear failure is shown in Fig. 4(a) when the stresses at the bolt cross-section are higher than 862 MPa (120 ksi). By monitoring von Mises stresses around the bolt lines net Shear-Bending Interaction failure mode were identified as shown in Fig. 4(b). The stresses around the bolt holes were examined in order to determine the bolt bearing failure mode. high stresses around the bolt hole are as shown in Fig. 4(c). To predict the failure mode of the SPS connection, forty-eight finite element models developed with ABAQUS produced the 7884 von mises stresses readings up to the ultimate load for each increment of load. The ultimate load around the bolt holes, at the mid-cross section of the bolt, and along the centerline of bolt which correspond to the first, second, and third outputs, respectively. LSTM can learn long-term dependencies in sequential data since it is specifically made to understand and memorise the von mises stresses with each increment of load of model inputs in sequential order.

5. Development of LSTM model

This study used the widely available MATLAB (R2017b) neural toolbox to develop an LSTM model for predicting the SPS connection failure mode. Choosing suitable input parameters is one of the most the essential aspects of LSTM modelling

An SPS connection's shear strength and mode of failure depend on multiple factors, including the span of the beam (L), depth of the web (d), thickness of the web (tw), depth of the tab (Lp), thickness of the tab (tp), number of bolts (N), number of bolt column (Nc), load distance (x), distance between the edge of the column to centerline of bolt (a), and load on beam (P). These factors are found by both experimental and finite element analysis (Satarkar *et al*. 2023). The von Mises stresses around bolt hole (first output, Sa), the von Mises stresses at cross section of bolt (second output, Sb), and the von Mises stresses in plate along centerline of bolt (third output, Sc) are outputs which are required to identify the failure mode of joints. Previous to this study, present authors have published their work wherein (Satarkar *et al.* 2023), average mutual information (AMI) method was used for the selection of inputs parameters. Seven neural network models were generated after trying with various input combinations using AMI values to study the performance of the model. Readers are directed to Satarkar *et al*. (2023) for more details. With reference to that work, the ANN7 model performed better than the other models. In this study same inputs and outputs of ANN7 model are used for development of LSTM model. Table 2 shows maximum and minimum values of the input and output parameters of ANN7 model. The input sequence contains 7884 von Mises stresses reading up to the ultimate load were generated from finite element analysis. The standard and efficient method for evaluating the model and modifying the parameters in machine learning algorithms is train/test splitting. Typically, the dataset is split into two sections: the training set (1-5519 rows) and the test set (5520 – 7884 rows). The former is used to train the model, whereas the latter is used to test the trained model's performance. The model in this study was trained using MATLAB's default batch-handling approach (wherein the entire data is used as batch) for sequence networks rather than manually setting a batch size. The best combination of hyperparameters can be found by adjusting the model based on the prediction performance in the test set.

This work followed a widely used approach of dividing the total data into two portions: 70% of the data for training and 30% of the data for testing. The network thus developed was trained by Adam optimizer which is derived from adaptive moment estimation. During testing, the network's performance was evaluated both quantitatively using the correlation coefficient (R), mean absolute

Table 2 Maximum and minimum values of the input and output parameters of ANN7 model

Input / target parameters	Max Value	Min Value	Unit
Inputs			
Load Distance (x)	8255	762	Mm
Load (P)	2670	0	kN
Number of bolt column (Nc)	2	1	-
Number of bolt (N)	8	3	-
Depth of shear plate (Lp)	610	230	Mm
Outputs			
Von Mises stresses around bolt hole (Sa)	0.4842	0.01679	kN/mm^2
Von Mises stresses at cross section of bolt (Sb)	1.03952	0.02436	kN/mm^2
Von Mises stresses in plate along Centreline of bolt (Sc)	0.4755	0	kN/mm^2

error (MAE), and root mean squared error (RMSE), and qualitatively using a scatter plot between the target and output.

The number of LSTM layers, BiLSTM layer, neuron number in each layer, and the optimizer are some of the key parameters that may have an impact on the final performance prediction (Qiao *et al.* 2021, Wang *et al*. 2022). This study finds the optimal number of LSTM layers according to the models with the highest accuracy, and then determines the best optimizer and the ideal number of LSTM neurons. The accuracy difference can be found under different layers with 1, 2, 3 and 4 LSTM layers. The architecture of LSTM layers used in this study is shown in Fig. 3. To evaluate the impact of hidden units on the LSTM performance, this research designs the cases of different unit numbers from 10 to 100 with an increase of 10 and 100 to 300 with an increase of 50. Learning rate was set as 0.01. For the training process in models with different layers, the training epochs were set from 50 to 500, with an increase of 50. In order to prevent overfitting during model training, a dropout layer was also inserted after each LSTM hidden layer, its value was set as 0.2 (Zhang *et al.* 2019). Using the same number of neurons as per the LSTM layer, the BiLSTM layer is placed before the fully connected layer. To train the LSTM model, the loss function used Mean Squared Error (MSE). The models were trained different number of epochs and training was stop when the results for training where the best.

6. Results and discussion

In this study, an LSTM network is used to compare conventional ANN (Satarkar *et al.* 2023) for failure mode prediction. The layer numbers and the hidden units of the LSTM architecture, are the two parameters that may affect the prediction performance of the LSTM network. In this section the influence of LSTM architecture (layer numbers and hidden units) and training dataset on the LSTM performance will be presented and discussed. The correlation coefficient, RMSE and the computational time were selected to evaluate the performance.

6.1 Optimization of LSTM layers and LSTM hidden units

The neural network's architecture and hyperparameter selections determine how well the neural network prediction model performs. Neural network performance is highly dependent on the precise initialization of hyperparameters, including the number of LSTM layers, the quantity of hidden neurons, the learning rate, etc. The number of hidden neurons indicates the network's correlation complexity, whereas the learning rate finds the network's rate of weight update. When the number of hidden neurons in the network is too high, the overfitting issue could arise. Instead of understanding the discipline hidden behind the training samples, the over-fitted network has a tendency to memorise every feature of the training samples, even unrepresentative ones. The over-fitted network thus fits poorly on the testing set however performs well on the training set.

To evaluate the layer numbers and hidden units in layer, this research designed four different cases from 1 layer to 4 layers. The number of hidden units used in each layer from 10 to 100 with an increase of 10 and 100 to 200 with an increase of 50. For the training process in models with different layers, the training epoch is set from 50 to 250, with an increase of 50. The correlation coefficient (r) between the LSTM modelled and FEA modelled values is better in the first three cases (1 layer, 2 layers, and 3 layers) compared to the fourth case (4 layers). Fig. 5 shows that the correlation coefficient is maximum when there are three layers and it improves as the number of epochs increases. The results also show that an increase in the number of hidden neurons in the LSTM layer has an adverse effect on the correlation coefficient because more hidden neurons increase the complexity of the model. Similar correlation coefficient plots are also observed in other cases as well (using 1, 2 and 4 layers) which are not shown here due to paucity of space.

When there are three layers the RMSE is the lowest compared to other layers as shown in Fig. 6, and it decreases as the number of epochs increases. It also demonstrates that the RMSE value reduces up to 150 neurons, and that the value grows with the number of neurons. When the hidden neurons vary from 50 to 150, RMSE fluctuates in a small range, while when the hidden neurons are out of the range, the RMSE increases significantly.

In addition, the computational times of training significantly increase with the increase in the number of layers (Fig. 7). The computational time increases smoothly with the growing hidden units and by increasing layer. However, Fig. 7 showed that time increases from Layer 1 to Layer 3, with a significant drop-in time after Layer 3. It proves that adding more hidden neurons speeds up convergence but increases the network's training time.

Table 3 displays the best outcome of LSTM models for each layer, in accordance with the aforementioned discussion and graph. Herein, one to three layered LSTM networks with different number of hidden neurons are constructed. The r, RMSE, and MAE are used to assess the performance of well-trained LSTM networks. As the number of LSTM layers increases from one to three, improvements in accuracy and stability are observed. It can be noted that, the accuracy of 3 layered LSTM model is the highest. After quantitative analysis of LSTM models, Figs. 8(a)-8(c) shows the scatter plot of three-layer LSTM model for 1st (von mises stresses around bolt hole), 2nd (von mises stresses at cross section of bolt) and 3rd (von mises stresses in plate along centreline) outputs, respectively. A good correlation coefficient between the observed and predicted values indicates the balanced scatter patterns between the observed and predicted values. However, the scatter shows a low level of prediction accuracy for the 1st output. For the low value of observed stress at 0.25 kN/mm2, the stresses predicted were increasing. Also there seems to be an under-prediction. The stresses predicted in the second output proved to be overpredicted; in contrast, the third output showed a balance between over and underprediction.

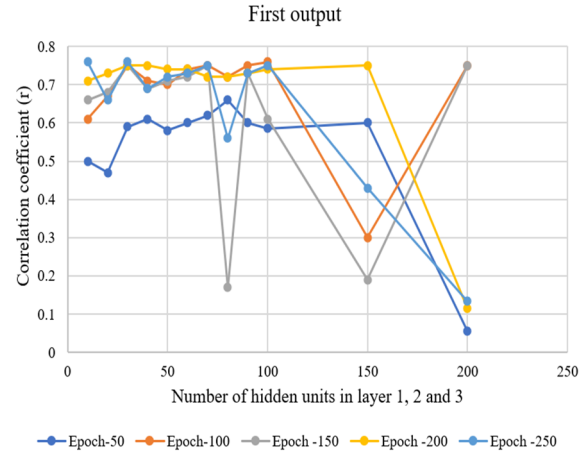

(a) First output

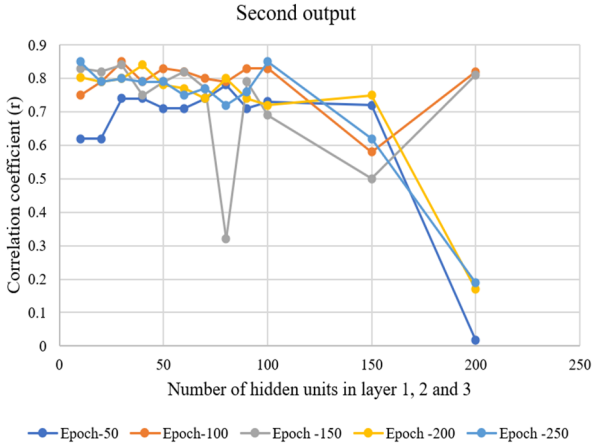

(b) Second output

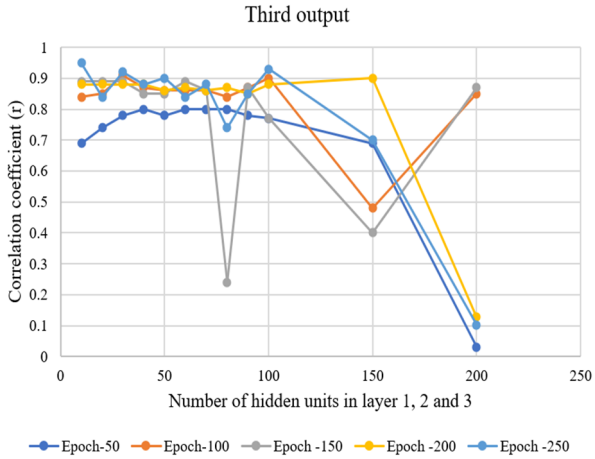

(c) Third output

Fig. 5 Correlation coefficient using three LSTM layers

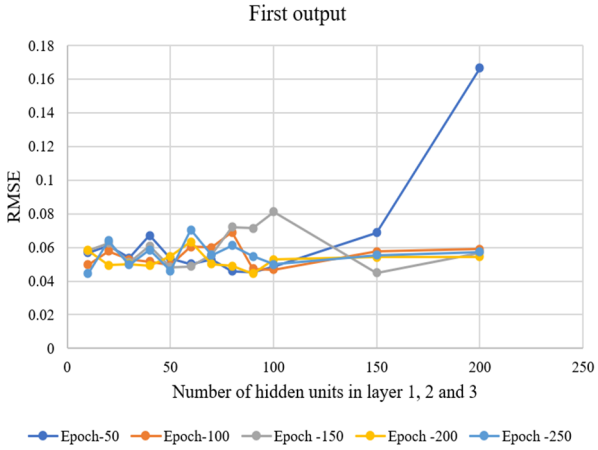

(a) First output

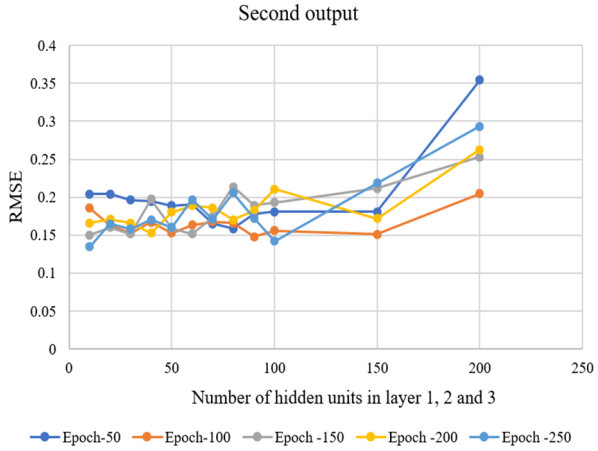

(b) Second output

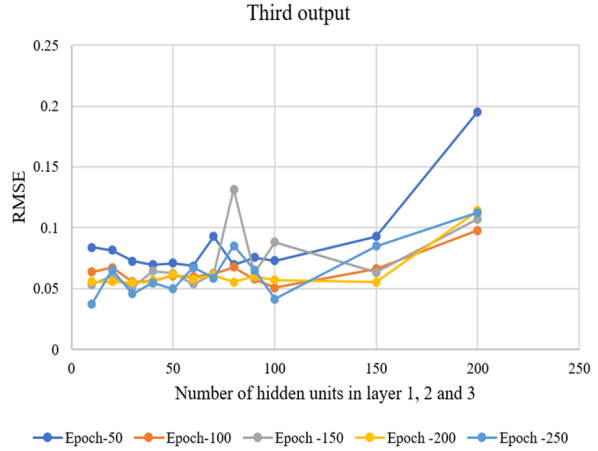

(c) Third output

Fig. 6 RMSE using three LSTM layers

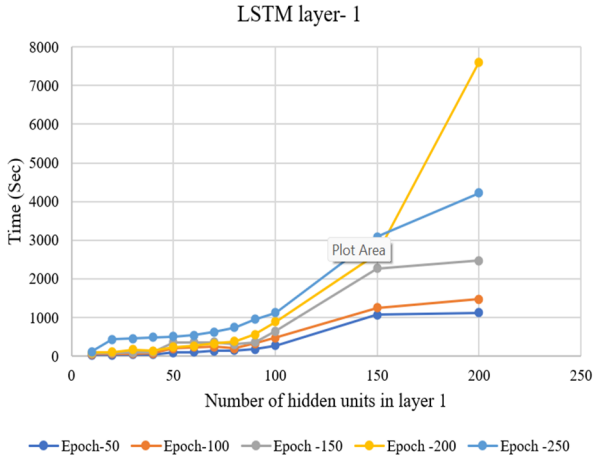

(a) Layer 1

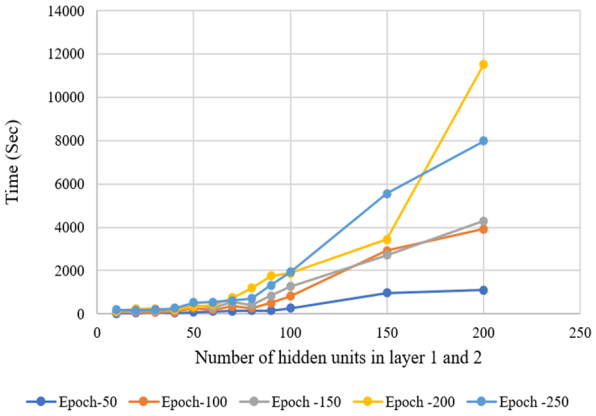

(b) Layer 2

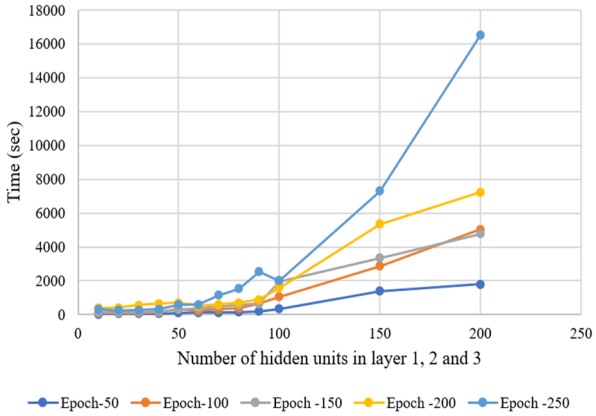

(c) Layer 3

Fig. 7 Computational time under different hidden neuron and layer numbers

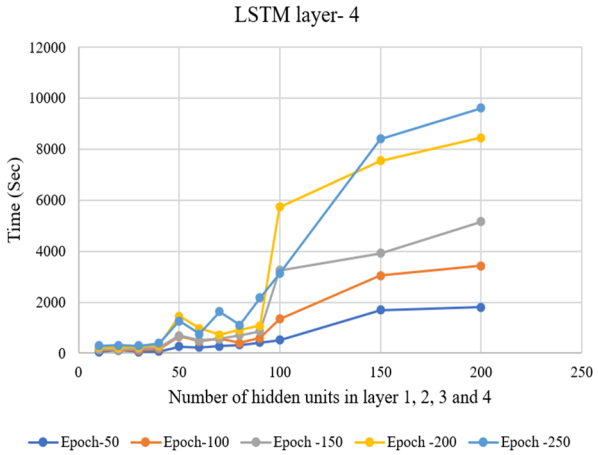

(d) Layer 4

Fig. 7 Continued-

6.2 Comparison of ANN and LSTM

In this study same parameters were used for ANN and LSTM networks. As the number of LSTM layers increases from one to three, improvements are seen in accuracy and stability. It can be noted that, the accuracy of 3 layered LSTM model is high. The comparison between the conventional ANN (Satarkar *et al.* 2023) and three-layered deep LSTM network results is illustrated in Table 4. The table lists the comparison of RMSE, MAE and correlation coefficient (r). Table 4 shows the RMSE and r values of ANN model are better than LSTM network. ANN outperformed the LSTM outcomes in terms of performance and convergence speed. This indicates that the ANN network can effectively generalise the data.

It may be noted that, the average time consumed to analyse deep LSTM network was around one hour using the Microsoft operating system, I5 processor, and 16 GB RAM. The training and testing of the ANN models took an average of six seconds. The findings of this research show that both the ANN and LSTM models can accurately detect failure modes in SPS connections. ANN outperformed the LSTM outcomes in terms of performance, accuracy, error measures and convergence speed. This indicates that the ANN network can effectively generalise the data. Thus, it can be said that ANN models are sufficient for this type of data if they produce better outcomes in a shorter amount of time compared to its counterpart of deep learning tools.

This result indicates that the deep-learning architectures are not essential for modelling the failure mechanisms which are considered in the present work. Specifically, the connections failure progression shows comparatively direct nonlinear behaviour with small long-term dependency. Short-term load-stress data is adequate for good prediction since the response of the structure changes quickly as the connection gets closer to failure. In these circumstances, a conventional ANN, which was developed to understand static nonlinear input-output relationships, either matches or surpasses the predictive ability of LSTM models. Similar findings have been documented in the SHM literature, where simpler ANN architectures outperform deeper or sequence-based models in situations when datasets are small or degradation pattern is not highly time-dependent (Ahmed *et al.* 2022). The LSTM is more adaptable in situations when failure

Table 3 Performance of LSTM models

Case	Parameters			Predicted output									Time (Sec)
				First output			Second output			Third output			
	Number of hidden unis in LSTM layer	Number of hidden unis in biLSTM layer	No of Epochs	r	RMSE	MAE	r	RMSE	MAE	r	RMSE	MAE	
Layer 1	70	70	100	0.76	0.0465	0.02	0.85	0.1364	0.0222	0.91	0.0481	0.0015	249
Layer 2	200	200	250	0.76	0.0477	0.01	0.86	0.1292	0.0145	0.93	0.0425	0.0118	5544
Layer 3	**10**	**10**	**250**	**0.76**	**0.0444**	**0.0029**	**0.85**	**0.1346**	**0.0006**	**0.95**	**0.0375**	**0.0078**	**324**
Layer 4	10	10	250	0.77	0.0561	0.03	0.82	0.1624	0.0198	0.9	0.0525	0.0119	300

Table 4 Comparison of ANN and three-layered LSTM model

	RMSE		MAE		r	
Outputs	ANN	LSTM	ANN	LSTM	ANN	LSTM
First output	0.0406	0.0444	0.0175	0.0029	0.83	0.76
Second output	0.1108	0.1346	0.0091	0.0006	0.88	0.85
Third output	0.0500	0.0375	0.0083	0.0078	0.91	0.95

occurs over several cycles, such as cumulative damage and complex repeated degradation processes, because it records sequential changes in the response signals. In accordance with results from earlier SHM research studies, temporal or recurrent models perform well when structural responses show clear progression patterns across time. As a result, comparing ANN and LSTM improves comprehension of how various ML architectures function under various structural behaviours characteristics. Therefore, the results demonstrate that ANN and LSTM models provided sound techniques for detecting SPS connection failure modes. The LSTM provides comparable strengths by identifying sequential response patterns and offering a framework for future applications with more complex time-evolving degradation, whereas the ANN achieved a bit superior numerical accuracy because of the dataset's limits on temporal dependency.

7. Conclusions

The aim of this work was to create deep LSTM models in order to predict the failure mode of SPS connections according to von Mises stress values. The finite element method was used to generate the data needed for the development of the LSTM model. Using code AISC (2010), 48 SPS connections with different configurations were designed, failure analysis by FEM was performed using ABAQUS.

The LSTM model used the same inputs as the conventional ANN model (ANN7). With reference to previous work ANN7 model performed better than the other six models. The optimal architecture for LSTM models was determined by changing the hyperparameter. The performance of predictions is considerably affected by the LSTM architecture. In this study, an architecture with three LSTM layers, 10 hidden units in LSTM layers, and BiLSTM layers using 250 epochs achieved the best prediction results. It took 1 hour to complete the training. Low RMSE and MAE

values are obtained by increasing layers from one to three, however beyond layer three, RMSE and MAE values begin to rise. The method accurately predicts multiple failure modes and effectively presents stress behaviour. Early-stage failure detection is made possible without a requirement for complicated post-processing or visual image data by using stress history as model input. Furthermore, the technology can be combined with parametric FE simulations for extensive reliability evaluations and provides computational efficiency.

The traditional neural network, ANN, was compared with the deep learning network, LSTM. The ANN models perform better than the LSTM model, according to the values of the statistical parameters RMSE, MAE, and r. It is important to note that if ANN models produce better results in a shorter amount of time, then deep learning or other complex analysis processes are not that essential to these types of problems. However, it may be said that these results are based on just one exercise and perhaps with different set of loading conditions, dimensions the results may vary. This research has a few of shortcomings apart from its advantages. Future research should include experimental datasets to improve adaptability, as the model's predictions are only based on stress data obtained by finite element analysis. The classification of failure mode is limited to the predetermined categories utilised in this research; connections that showed secondary or combined failure mechanisms were not considered. Future studies should concentrate on expanding to different steel connection arrangements, incorporating more failure types and integrating with experiment analysis.

Acknowledgments

This research did not receive any specific grant from funding agencies in the public, commercial, or not-for profit sectors.

References

ABAQUS standard user's manual. (2017), Hibbitt, Karlsson and Sorenson, Inc.

Abambresa, M. and Lantsoghtc, E. (2020), "Neural network-based formula for shear capacity prediction of one-way slabs under concentrated loads", *Eng. Struct.*, **211**, 1-9. https://doi.org/10.36227/techrxiv.12672191.v1.

Ahmed, M.Y., Karim, A.E. and Mohamed, E.E. (2022), "Prediction of ultimate shear strength and failure modes of R/C ledge beams using machine learning framework", *Struct. Monit. Maint.*, **9**(4), 337-357. https://doi.org/10.12989/smm.2022.9.4.337.

Allahyari, H., Iman, M., Nikbin, Saman, R.R. and Heidarpoura, A. (2018), "A new approach to determine strength of Perfobond rib shear connector in steel-concrete composite structures by employing neural network", *Eng. Struct.*, **157**, 235-249. https://doi.org/10.1016/j.engstruct.2017.12.007.

American Institute of Steel Construction, AISC, (2010), Manual of Steel Construction. 14th Ed.

Ashakul, A. (2004), "Finite element analysis of single plate shear connections", Doctor of Philosophy Dissertation, Virginia Polytechnic Institute and State University, Blacksburg, Virginia.

Bakhshi, Ostadkalayeh, F., Moradi, S., Asadi, A., Nia, A.M. and Taheri, S. (2023), "Performance improvement of LSTM-based deep learning model for streamflow forecasting using Kalman filtering", *Water Resour. Management*, 1-17. https://doi.org/10.1007/s11269-023-03492-2.

Bergen, K.J., Johnson, P.A., de Hoop, M.V. and Beroza, G.C. (2019), "Machine learning for data-driven discovery in solid Earth geoscience", *Science*, **80**(363). https://doi.org/ 10.1126/science.aau0323.

Butta, F.M., Hussain, L., Jafria, S.H.M., Alshahranie, H.M., Al-Wesabi, F.N., Lone, K.J., Elsayed M.T.E.D.

and Duhayyim, M.A. (2022), "Intelligence based accurate medium and long term load forecasting system", *Appl. Artif. Intel.,* **36**, 2066-2089. https://doi.org/10.1080/08839514.2022.2088452.
Cha, Y.J., Mostafavi, A. and Benipal, S.S. (2023), "DNoiseNet: Deep learning-based feedback active noise control in various noisy environments", *Eng. Appl. Artif. Intel.*, **121**. https://doi.org/10.1016/j.engappai.2023.105971.
Choe, D.E., Kim, H.C. and Kim, M.H. (2021), "Sequence-based modeling of deep learning with LSTM and GRU networks for structural damage detection of floating offshore wind turbine blades", *Renew. Energy*, **174**, 218-235. https://doi.org/10.1016/j.renene.2021.04.025.
Creech, D.D. (2005), "Behaviour of single-plate shear connections with rigid and flexible supports", Master's Thesis, North Carolina State University, Department of Civil and Environmental Engineering, Raleigh, NC.
Dais, D., Bal, I.E., Smyrou, E. and Sarhosis, V. (2021), "Automatic crack classification and segmentation on masonry surfaces using convolutional neural networks and transfer learning", *Automat. Constr.*, **125**. https://doi.org/10.1016/j.autcon.2021.103606.
Daniel, J. and Ruffley. (2011), "A finite element approach for modeling bolted top-and-seat angle components and moment connections", Master of Science thesis, University of Cincinnati, College of Engineering. https://doi.org/10.1201/b11396-18.
Fils, P., Jang, S. and Sherpa, R. (2021), "Field implementation of low-cost RFID-based crack monitoring using machine learning", *Struct. Monit. Maint.*, **8** (3), 257-278 https://doi.org/10.12989/smm.2021.8.3.257.
Gong, Y. (2010), "Plastic behaviour of shear tabs welded to flexible wall support", *J. Struct. Eng.*, 1197-1204. https://doi.org/10.1061/(ASCE)ST.1943-541X.0000223.
He, Y. and Chen, Q. (2023), "Construction and application of LSTM-based prediction model for tunnel surrounding rock deformation", *Sustainability*, **15** (8), 1-12. https://doi.org/10.3390/su15086877.
Ho, D., Luu, T.T. and Pham, M.N. (2022), "Nondestructive crack detection in metal structures using impedance responses and artificial neural networks", *Struct. Monit. Maint.*, **9** (3), 221-235. https://doi.org/10.12989/smm.2022.9.3.221.
Hochreiter, S. and Schmidhuber, J. (1997), "Long short-term memory", *Neural Comput.*, **9**(8), 1735-1780. https://doi.org/10.1162/neco.1997.9.8.1735.
Kirsten, A. and Metzger, B. (2006), "Experimental verification of a new single plate shear connection design model", Master of Science thesis, Blacksburg, VA.
Kotsovou, G.M., Cotsovos D.M. and Lagaros, N.D. (2017), "Assessment of RC exterior beam-column Joints based on artificial neural networks and other methods", *Eng. Struct.*, **144**(4), 1-18. https://doi.org/10.1016/j.engstruct.2017.04.048.
Lima, L.R.O., Vellasco, P.C.G., Andrade, S.S.A.L. and Silva, J.G.S. (2005), "Neural networks assessment of beam-to-column joints", *J. Braz. Soc. Mech. Sci. Eng.*, **27**(3). https://doi.org/10.1590/S1678-58782005000300015.
Limbachiya, V. and Shamass, R. (2021), "Application of artificial neural networks for web-post shear resistance of cellular steel beams", *Thin Wall Struct.*, **161**, 1-9. https://doi.org/10.1016/j.tws.2020.107414.
Liu, H., Ding, Y.L., Zhao, H.W., Wang, M.Y. and Geng, F.F. (2020), "Deep learning-based recovery method for missing structural temperature data using LSTM network", *Struct. Monit. Maint.*, **7**(2), 109-124. https://doi.org/10.12989/smm.2020.7.2.109.
Mandic, D.P. and Chambers, J. (2001), "Recurrent neural networks for prediction: Learning algorithms", *Architect. Stab.*, https://doi.org/10.1002/047084535X.
Mansour, M.Y., Dicleli, M., Lee, J.Y. and Zhang, J. (2004), "Predicting the shear strength of Reinforced concrete beams using artificial neural networks", *Eng. Struct.*, **26**, 781-799. https://doi.org/10.1016/j.engstruct.2004.01.011.
Mazloom, M., Afkar, H. and Pourhaji, P. (2018), "Assessing the ductility of moment frames utilizing genetic algorithm and artificial neural networks", *Struct. Monit. Maint.*, **5**(4), 445-461. https://doi.org/10.12989/smm.2018.5.4.445.
Medsker, L. and Jain, L. C. (1999), "Recurrent neural networks: Design and applications", CRC Press.
Murad, Y.Z., Hunifat, R. and Bodour, W.A. (2020), "Interior reinforced concrete beam-to-column joints

subjected to cyclic loading: shear strength prediction using gene expression programming", *Case Studies Constr. Mater.*, **13**, 1-9. https://doi.org/10.1016/j.cscm.2020.e00432.

Nguyen, C.U., Huynh, T.C. and Kim, J.T. (2018), "Vibration-based damage detection in wind turbine towers using artificial neural networks", *Struct. Monit. Maint.*, **5**(4), 507-519. https://doi.org/10.12989/smm.2018.5.4.507.

Nguyen, T.T., Ahn, Y., Lee, S., Lim, B.T.H. and Oo, B.L. (2025), "Managing and predicting embodied carbon emissions for ready-mix concrete products using model-agnostic meta-learning technique", *J. Build. Eng.*, 111. https://doi.org/10.1016/j.jobe.2025.113554.

Qiao, D., Li, P., Ma, G., Qi, X., Yan, J., Ning, D. and Li, B. (2021), "Realtime prediction of dynamic mooring lines responses with LSTM neural network model", *Ocean. Eng.*, **219**, 108368. https://doi.org/10.1016/j.oceaneng.2020.108368.

Ranjbar, I. and Toufigh, V. (2022), "Deep long short-term memory (LSTM) networks for ultrasonic-based distributed damage assessment in concrete", *Cement Concrete Res.*, **162**, 107003, 1-16. https://doi.org/10.1016/j.cemconres.2022.107003.

Razavi, M. and Hadidi, A. (2020), "Assessment of sensitivity-based FE model updating technique for damage detection in large space structures", *Struct. Monit. Maint.*, **7**(3), 261-281. https://doi.org/10.12989/smm.2020.7.3.261.

Rosebrock, A. (2017), "Deep learning for computer vision with python", www.pyimages earch.com.

Satarkar, P.R., Londhe, S.N., Dixit, P.R. and Mohamed, F.S. (2023), "Modelling the behaviour of extended shear tab connection using artificial neural network", *Asian J. Civil Eng.*, **24**, 2767-2782. https://doi.org/10.1007/s42107-023-00673-7.

Savino, P. and Tondolo, F. (2021), "Automated classification of civil structure defects based on convolutional neural network", *Struct. Civ. Eng.*, **15**(2), 305-317. https://doi.org/10.1007/s11709-021-0725-9.

Sharma, S. and Sen, S. (2023), "Real-time structural damage assessment using LSTM networks: regression and classification approaches", *Neural Comput. Appl.*, **35**(1), 557-572. https://doi.org/10.1007/s00521-022-07773-6.

Sherman, D.R. and Ghorbanpoor, A. (2002), "Design of extended shear tabs", Final Report to American Institute of Steel Construction AISC: University of Wisconsin- Milwaukee, USA.

Singh, G.K., Patel, K.A., Chaudhary, S. and Nagpal, A.K. (2021), "Methodology for rapid estimation of deflections in two-way rein forced concrete slabs considering cracking", *Pract. Period. Struct. Design Constr. ASCE*, **26**(2), 1-10. https://doi.org/10.1061/(ASCE)SC.1943-5576.0000568.

Smagulova, K. and James, A.P. (2019), "A survey on LSTM memristive neural network architectures and applications", *Eur. Phys. J. Spec. Top*, **228**, 2313-2324. https://doi.org/10.1140/epjst/e2019-900046-x.

Suleiman, M.F. (2013), "Non-linear finite element analysis of extended shear tab connections", Ph.D. Dissertation, University of Cincinnati, Department of Civil and Architectural Engineering and Construction Management, Cincinnati, OH, USA.

Tang, Y.X., Lee, Y.H., Amran, M. Fediuk, R., Vatin, N., Kueh, A.B.H. and Lee, Y.Y. (2022), "Artificial neural network-forecasted compression strength of alkaline-activated slag concretes", *Sustainability*, **14**(9). https://doi.org/10.3390/su14095214.

Tariq, U., Ahmad, A., Suleiman, M. and Shaheen, M.A. (2022), "Prediction of steel flush end plate connection through Artificial Neural Networks (ANN)", *Proceedings of the 1st International Conference on Advances in Civil & Environmental Engineering*, University of Engineering & Technology Taxila, Pakistan.

Thilakarathna, P.S.M., Seo, S., Baduge, K.K., Lee, H., Mendis, P. and Foliente, G. (2020), "Embodied carbon analysis and benchmarking emissions of high and ultra-high strength concrete using machine learning algorithms", *J. Cleaner Product.*, **262**. https://doi.org/10.1016/j.jclepro.2020.121281.

Tohidi, S. and Sharifi, Y. (2016), "Load carrying capacity of locally corroded steel plate girder ends using artificial neural network", *Thin Wall Struct.*, **100**, 48-61. https://doi.org/10.1016/j.tws.2015.12.007.

Wang, Z., Qiao, D., Yan, J., Tang, G., Li, B. and Ning, D. (2022), "A new approach to predict dynamic mooring tension using LSTM neural network based on responses of floating structure", *Ocean. Eng.*,

249(2), 110905. https://doi.org/10.1016/j.oceaneng.2022.110905.
Xue, J. and Ou, G. (2021), "Predicting wind induced structural response with LSTM in transmission tower line system", *Smart Struct. Syst.*, **28**(3), 391-405. https://doi.org/10.12989/sss.2021.28.3.391.
Yan, J., Zhang, Y., Su, Q., Li, R., Li, H., Lu, Z., Lu, H. and Lu, Q. (2023), "Time series prediction based on LSTM neural network for top tension response of umbilical cables", *Mar. Struct.*, **91**, 103448, 1-18. https://doi.org/10.1016/j.marstruc.2023.103448.
Yura, J.A. and Summers, P.B. (1982), "The behaviour of beams subjected to concentrated loads", PMSFSEL Report No. 82-5 for the American Iron of Steel Institute, August, University of Texas, Austin, TX, USA.
Zhang, H. and Zhou, Y. (2023), "AI-based modeling and data-driven identification of moving load on continuous beams", *Fundamental Res.*, **3**, 796-803. https://doi.org/10.1016/j.fmre.2022.02.013.
Zhang, R., Chen, Z., Chen, S., Zheng, J., Buyukozturk, O. and Sun, H. (2019), "Deep long short-term memory networks for nonlinear structural seismic response prediction", *Comput. Struct.*, **220**, 55-68. https://doi.org/10.1016/j.compstruc.2019.05.006.
Zhao, G., Xing, K., Wang, Y., Qian, H. and Zhang, M. (2023), "Long short-term memory network for predicting wind-induced vibration response of lightning rod structures", *Buildings*, **13**(1256) 1-22. https://doi.org/10.3390/buildings13051256.
Zhao, J., Ivan, J.N. and DeWolf, J.T. (1998), "Structural damage detection using artificial neural networks", *J. Infrastruct. Syst. ASCE*, **4**(3), 93-101. https://doi.org/10.1061/(ASCE)1076-0342(1998)4:3(93).